Catchment properties shape seasonal variation in groundwater- surface water interaction – geogenic silicate as a proxy for hydrological turnover induced mixing

Lars Bäthke[1] and Tobias Schuetz[1]

[1] Department of Hydrology, Faculty of Regional and Environmental Sciences, University of Trier, Trier, Germany

Corresponding author:

Lars Bäthke (baethke@uni-trier.de) and Tobias Schuetz (tobias.schuetz@uni-trier.de)

Key Points:

- Site specific decoupling of hydraulic gradients and reach scale absolute discharge changes from hydrological turnover.
- Seasonal variation of hydrological turnover compared to site specific catchment drainage behaviour.
- Geogenic silicate concentrations can serve as a proxy for hydrological turnover induced mixing with subsurface waters.

Abstract

The cumulative and bidirectional groundwater-surface water (GW-SW) interaction along a stream is defined as hydrological turnover (HT) influencing solute transport and source water composition. However, HT proves to be highly variable, producing spatial exchange patterns influenced by local surface- and groundwater levels, geology, and topography. Hence, identifying factors controlling HT in streams poses a challenge. We studied the spatiotemporal variability of HT processes at a third order tributary of the river Mosel, Germany at two different stream reaches over a period of two years. Additionally, we sampled for silicate concentrations in the stream as well as in the near-stream groundwater. Thus, creating snapshots of the boundary layer between ground- and surface water where turnover induced mixing occurs. We characterize reach specific drainage behavior by utilizing a delayed/base flow separation analysis for both reaches. The results show a site-specific negative correlation of HT with discharge, while hydraulic gradients and reach scale absolute discharge changes correlating with HT only at the upstream site which is characterized by steeper hillslopes compared to the downstream section. Analyzing the variation of silicate concentrations between stream and wells shows that in-reach silicate variation increases significantly with the decrease of HT under groundwater dominated flow conditions.. In Summary, our results show that discharge shapes the influence of HT on solute transport as visualized by silicate variations. Yet, reach specific drainage behavior shapes seasonal states of groundwater storages and thus, can be an additional control of HT magnitudes, influencing physical stream water composition throughout the year.

1 Introduction

The process of groundwater-surface water (GW-SW) interaction along river corridors integrates the movement of water masses between the near stream groundwater aquifer, the riparian zone and the stream channel (Payn et al., 2009; Ward et al., 2013, 2019), with the hyporheic zone as the boundary layer between stream and groundwater which is highly variable in dimension (Wondzell et al., 2011). The exchange between GW and SW along streams needs to be addressed as bidirectional, consisting of gross gains and losses influencing a significant proportion of stream flow (Payn et al., 2009; Covino et al., 2011). In this context, the cumulative effect of bidirectional fluxes is understood as a hydrological turnover (HT), shaping source water composition (Covino et al., 2011; Mallard et al., 2014) in conjunction with solute transport and controlling in-stream ecological functions (Covino et al., 2011; Jimenez-Fernandez et al., 2021) as well as stream chemical signatures (Jähkle et al., 2022). Base flow is often assumed to be geochemically constant in accordance with the underlying geology (e.g., Klaus & McDonnel, 2013), while the variability in stream chemistry is hinting towards variety in source waters and contributing storages in the subsurface (Payn et al., 2012; Blumenstock et al., 2015). HT processes dampen the spatially distinct contributions of source areas forming streamflow and its chemical signatures (Schuetz et al., 2016) and thus revealing the recycling of water between the stream and the underground (Covino et al., 2011; Mallard et al., 2014). The simultaneous process of losing and gaining water has large implications on the perspective towards stream deprived groundwater recharge and modifies discharge signals in watersheds. Hence, net changes of discharge are insufficient to characterize GW-SW interaction along streams (Covino et al., 2011; Mallard et al., 2014). There are several features known to influence GW-SW interaction, namely the hydrologic forcing and the geomorphic setting (Ward et al., 2019). Hydrologic forcing summarizes the temporal variation of catchment wetness, groundwater storage states (Ward et al., 2013; Dudley-Southern & Binley, 2015; Malzone et al., 2016) and diverging drainage behavior of different geologies (e. g. Payn et al., 2012, Stoelzle et al., 2014) in combination with the magnitude of the actual stream flow (Payn et al., 2009; Voltz et al., 2013; Ward et al., 2013; Schmadel et al., 2017) and thus, distinct water levels on the local scale. In sum, it shapes the temporal participation of different flow paths in HT. Flow paths dominated by geomorphic setting are governed by hydraulic gradients and thus, more persistent in time (Schmadel et al., 2017). Thus, also HT is subject to hydrologic forcing and the geomorphic setting and presents itself as variable in time and space, with multiple influencing factors on multiple scales (Payn et al., 2009). On smaller scales stream morphologies, with reach specific pool and riffles sequences, rock outcrops, bankstorage and transient storages or locally focused GW discharge areas (Schuetz & Weiler, 2011) govern GW-SW interaction to a large degree (e.g. Bencala & Walters, 1983; Runkel et al., 1998, 2002; Bencala, 2000; Gückner & Böchat, 2004). Spatial variations in losing or gaining river segments (Zimmer et al., 2016) show the effect of different hyporheic flow pathways from small to larger scales (Cardenas, 2008; Ward et al., 2017). Also, on smaller scales seasonal effects such as biofilm formation (Arnon et al., 2010, 2013; De Falco et al., 2018) and bioturbation (Battin et al., 2008, 2016) are possible sources of the variability in GW-SW interaction over time. Altogether, these processes induce the spatial and temporal variability of HT processes. However, reach specific features on, i.e hillslope topography, geology, vegetation, and valley bottom structure influence streamflow dynamics and GW-SW interaction (Bergstrom et al., 2016; Jähkel et al., 2022; Jimenez-Fernadez et al., 2021) and studies measuring HT at the reach and catchment scale show that discharge can explain the variance in HT quite well (Covino et al., 2011; Mallard et al., 2014).

Few methods are available to study GW-SW interaction from scales smaller than 1 m up to more than several hundred meters. Utilizing e.g. electrical conductivity in analysis of bank filtration (Cirpka et al., 2007), water temperature and hydraulic gradient-based approaches (e.g. Kalbus et al., 2006; Schmidt et al., 2006; Schmitgen et al., 2021), often in combination with differential gauging (e.g. Ruehl et al., 2006). Hydrograph separation methods based on tracers such as stable water isotopes or silicate are frequently used to differentiate between quick and slow flow, thus shedding light on slow flow signals (e.g. Penna et al., 2015; Klaus & McDonnell 2013; Uhlenbrook & Hoeg, 2003; Wels et al., 1991). However, mass balance-based slug tracer injections in combination with dilution gauging is up till now, the only available method of quantifying gross gains and losses resulting in HT estimation of larger stream segments (Payn et al., 2009; Covino et al., 2011; Mallard et al., 2014; Jimenez-Fernadez et al., 2021; Jäkhel et al., 2022).

In numerical groundwater models, surface water levels are commonly used as a static or variable boundary condition (Staudinger et al., 2019). A few studies only, try to explore spatial effects of GW-SW interaction on groundwater fluxes and indirect GW recharge on the scale of an alluvial aquifer section using hydrodynamic numerical groundwater models (e.g. Wöhling, 2021). The consideration of HT on the catchment scale in hydrological models has been tested currently (Staudinger et al., 2021), using an additional catchment scale exchange bucket. Mallard et al. (2014) presents an empirical equation based on discharge magnitudes and drainage area to scale up observed HT to the catchment scale and along the stream network. While both are straightforward approaches, neither of them considers site-specific stable geomorphic forcing nor the temporal variations of the hydrological forcing and thus might be restricted in transferability to other catchments. Up until now, no sufficient and transferable model concept exists to allow the consideration of HT processes for hydrological models applied on the catchment scale.

In previous studies, HT was analyzed in conjunction with large scale valley structure transition and stream water balance dynamics in summer resection establishing that even under net gaining conditions bidirectional flow is of significance (Payn et al., 2009). Covino et al., (2011) showed

that the hydrologic exchanges occurring along stream reaches may not be properly characterized by net changes in Q, identifying the HT process as having implications for source water contribution, and suggesting that besides watershed structure and network geometry additional factors such as groundwater recharge and aquifer storage state control HT. Bidirectionality in GW-SW interaction is also apparent in the work of Zimmer et al. (2016), suggesting that ephemeral and intermittent streams temporally can act as both sources and sinks for groundwater across humid headwater landscapes and independent of deep groundwater contributions run-off can be produced at low storage states. Hence, these processes need to be better understood, supporting the development of improved HT modelling approaches on the catchment scale.
Only limited numbers of HT observations have been published in the international literature so far (e.g. Payn et al., 2009; Covino et al., 2011; Mallard et al., 2014; Jimenez-Fernadez et al., 2021; Jäkhel et al., 2022). Most of them either limited in scale with consistent reach segments of about 100 meters (Jimenez-Fernadez et al., 2021, Jäkhel et al., 2022) covering two seasons, or observation periods capture four months in the same season, respectively (Payn et al., 2009; Covino et al., 2011; Mallard et al., 2014). Reflecting these limitations, we explore the effect of opposing geomorphic settings and seasonal variations in catchment storages as controls of HT in two ~ 500 m reaches of the same catchment with distinct differences in morphological features. Additionally, addressing spatio-temporal variability and reach specific HT patterns, combining HT estimations with near stream groundwater silicate concentrations, hydraulic gradients and delayed flow hydrograph separation over a period of two years. Apparent silicate concentration in groundwater and surface water serves as a tracer for residence time. Due to its enrichment in the underground (e.g. Burns et al., 2003), it allows an analysis of turnover induced mixing between GW and SW with its implications on solute transport. In analyzing HT within the bigger framework of ever-changing hydrological forces over time and space, according to the following research questions:

1. *Are geomorphological valley properties linked with observable HT processes?*
2. *Is the seasonality of HT influenced by reach specific groundwater storage states?*
3. *Does HT has an effect on solute concentrations in near stream groundwater and what are the underlying mechanisms?*

2 Materials and Methods

2.1 Study Area

The Olewigerbach is a tributary of the river Mosel located south of the city of Trier (Rhineland-Palatinate; Germany). The catchment drains a 35 km^2 watershed with a total length of 14 km (Krein & Schorer 2000) and a mean channel with of 1.5 - 2 m. The altitude difference between headwater and mouth is about 300 m. The stream has a pluvial regime with a mean discharge of 250.6 ls^{-1} between 2010 and 2023. The catchment is geologically dominated by devonian schists with quartzite inclusions (Banzhaf & Scheytt 2009; Krein & Symader 2000). Therefore, groundwater permeability is limited to fissures and the soil layer. The catchment of the Olewigerbach covers different topographical features, allowing to choose two contrasting sites. The first study site is located at the upper reach “up-stream” at a height of approximately 300 m above sea level (Figure 1). The site is characterized by steep hillslopes with pastures and forest, the soil layer is shallow and dominated by clayey and silty material, with impermeable clay layers (Krein & Symader 2000). The second study site is located at the lower reach "down-stream" at a height of approximately 170 m above sea level (Figure 1). This site is less steep with a wider valley cross-section, characterized by a deeper loamy soil layer with clay pockets. The land use is dominated by pastures and forest at the meadow, vineyards, and forest at the slopes as well as settlement area (Banzhaf & Scheytt 2009; Krein & De Sutter 2001). In addition to that, the stream is stabilized by limestone blocks.

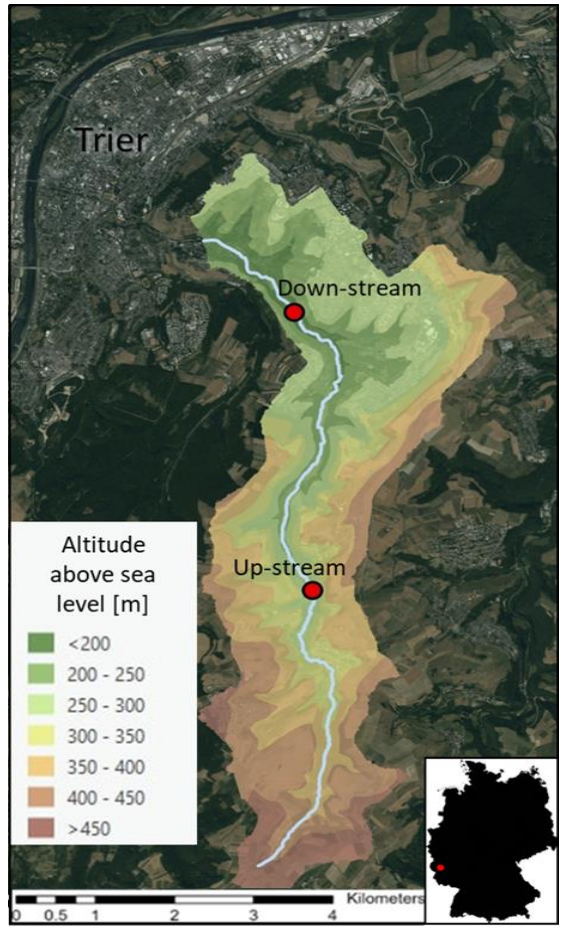

Figure 1. Site map of the Olewiger Bach catchment in the south of the city of Trier, Germany. Points marking the position of the two experimental reaches "Up-stream" and "Down-stream".

2.2 Experimental Setup

The study was carried out during the years from 2017-2022. Altogether, the data set is compiled of 133 differential discharge gauging campaigns (NaCl$^-$) and 270 stream- and groundwater samples. (Overview in Table 1). The collected field data includes streamflow magnitudes and groundwater levels at the head of the two reaches respectively. With water levels constantly logged in 5-min interval at both reaches from 2020 to 2022 (Orpheus Mini Level Logger, OTT). Groundwater levels were monitored at 5-min intervals in two wells at the head of each reach. At the down-stream reach (CTD-Diver, Van Essen) staring in March 2021, at the upstream reach (Orpheus Mini Level Logger, OTT) over the total observation period. We performed instantaneous tracer injections, similar to dilution gauging (Day, 1976), to analyze tracer breakthrough curves (BTCs). Several tracer injections were performed at various discharge conditions to determine appropriate mixing lengths (Kilpatrick & Cobb, 1985) at both study reaches, incorporating streamflow transitions as suggested in Payn et al. (2009). Considering the bidirectional flow of water masses between ground and surface water, as in the concept of HT (Covino et al., 2011; Payn et al., 2009), the loss of tracer mass is very likely during the mixing length. Therefore, the mixing lengths must be constant over time to ensure comparability of results, with the remaining variable to manage being the injected tracer mass. The upstream reach (~500 m) as well as the downstream reach (~500 m) were divided equally, resulting in three fixed tracer injection and sampling spots (Figure 2). During the campaigns, three WTW Multi devices were installed to log conductivity in series at 0 m, 250 m, and 500 m, respectively. In total, eight tracer injections were performed, four per study site. Slug injections of tracer started first at the base moving upward to the head of the reach. The first three injections at the study site yield BTCs to estimate discharges. During the campaigns, three WTW Multi devices were installed to log conductivity in series at 0 m, 250 m, and 500 m, respectively. In total, eight tracer injections were performed, four per study site. Slug injections of tracer started first at the base moving upward to the head of the reach. The first three injections at the study site yield BTCs to estimate discharges. Since EC probes were logging constantly, the dampened EC signals of the BTCs were recorded at all probes positioned downstream of the individual injection. Seven of the generated BTCs per tracer experiment and site were evaluated, amounting to 504 BTCs per site in total (Figure 2).

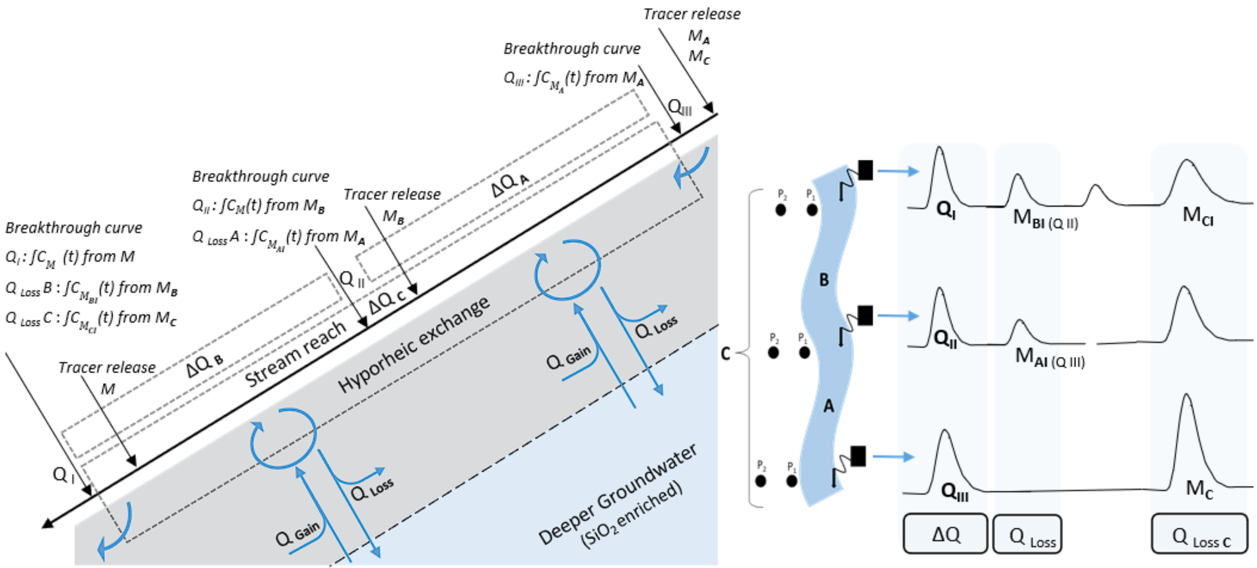

Figure 2. Left, summary of Tracer injections, breakthrough curve (BTC) measurements, discharge estimates, Tracer mass (M), Discharges are estimated from releases at base and head of the reaches ($Q_{I\text{-}III}$), calculating net exchange (ΔQ), mass recovered ($\int C_M$) used to estimate Gain and Losses (Q_{Loss}, Q_{Gain}). (Modified from Payn et al., 2009). Right, experimental setup, exemplary reach C, with sub-reaches as A, B, Groundwater wells as P_1 and P_2 at each measurement spot. Graphical description of logged BTCs utilized for Q and Q_{Loss} estimation.

Measurements were taken during discharge rates ranging from approximately 1 to 1008 ls^{-1}. The fourth tracer injection generated a BTC moving through the total reach, creating sufficient dampened EC signals at all three installed probes (Figure 2). This was ensured by doubling the tracer mass of the previous injections (constant mass per reach and experiment). The mass of the instantaneous injected pre-dissolved tracer (NaCl-) varied in the range of 50 g to 3000 g, depending on the apparent discharge and background electrical conductivity (EC). During low-flow conditions, the injection volume was chosen conservatively. BTCs with peak EC outside the range of 1.25 to 2.0 times background EC (typically 200 µS - 400 µS) were excluded or repeated. The produced BTCs were logged at 1s intervals, except during extreme low-flow conditions, when a 5 s resolution was utilized due to limitations in device storage capacity (Multi WTW). With BTCs derived from electrical conductivity curves minus background natural stream electrical conductivity per tracer release. Mass equivalent is calculated from conductivity curve via site and campaign day specific calibration for each measurement spot.

2.2.1 Hydrologic Turnover

The conducted tracer experiments provided BTCs to quantify changes in discharge along the reaches as well as gross gains and losses of stream water to and from groundwater. With discharge estimation:

$$Q_i = \frac{M_i}{\int_0^t C_{M_i}(t)dt} \tag{1}$$

Where Q_i is discharge at location *i*, M_i is initial tracer mass injected and $C_{M_i}(t)$ the integrated tracer concentration apparent in the BTC (Figure 2). All estimated discharges then are used to determine net discharge change ΔQ:

$$\Delta Q = Q_i - Q_{i-1} \tag{2}$$

With the upstream location *i-1*. Hydrological turnover (HT) estimation is based on the assumption of the loss of injected tracer mass along the channel equally represents the fractional loss of stream flow to the underground, not entering the stream channel again during the observation period (Payn et al., 2009; Covino et al., 2011). Hence, percent mass lost is equal to the fraction of initial Q lost over a reach (Covino et al., 2011):

$$Q_{Loss} = Q_{i-1} \frac{M_i - \int_0^t \mathrm{M}(t)dt}{M_i} \tag{3}$$

With Q_{i-1} discharge at the head and Q_{Loss} the water mass lost from head to base of the respective stream reach, assuming steady-state conditions throughout the window of detection (Figure 2a). Estimation of net Q and Q_{Loss} allow for determining Q_{Gain} and consequently for Q_{Turn} (Turnover) as follows:

$$\Delta Q = Q_{Gain} + Q_{Loss} \tag{4}$$

$$HT = |Q_{Loss}| + Q_{Gain} \tag{5}$$

Since 500 m reaches are larger than comparable setups in the literature (Payn et al., 2009; Jimenez-Fernadez et al., 2021; Jäkhel et al., 2022), we divided the study sites into two equidistant sub-reaches, resulting in three individual differential discharge gauging experiments. This enabled us to calculate HT parameters for the sub-reaches A and B and the total reach C separately. Subsequently, resulting in independent estimations of sub-reach and total reach Q, ΔQ, Q_{Loss}, Q_{Gain} and HT (Figure 2a). Thus, accounting for possible spatial discontinuity in GW-SW interaction at the reaches during all campaigns. To improve comparison of HT estimated at the "up-stream" and "down-stream" reach of the Olewigerbach catchment we performed a normalization, calculating HT as the fraction of total apparent discharge exchanged per meter of flow distance. Resulting in HT as [%/m] in the following. We compare the sub-reaches A and B to total reach C as follows:

$$C \sim A + B \tag{6}$$

Assuming that short term gains or losses in the sub-reaches as well as cross sub-reach turnover, cancel each other out, we tested for linear regression between the HT of total reach (C) and the sum of HT of the sub-reaches (A, B). In addition, we calculate ratios *r* of sub-reach contribution to HT,

$$r = \frac{A_{HT}}{B_{HT} + A_{HT}} \tag{7}$$

with values of r>0.5 showing that HT in sub-reach A is larger than HT in sub-reach B and values < 0.5 showing that HT in sub-reach B is more pronounced than HT in sub-reach A.

2.2.2 Silicate variability as a tracer for GW involvement in HT processes

Concentrations of silicate (SiO^2) are low in rainfall becoming higher in water infiltrating the underground because of dissolution or interaction with silicate bearing minerals in the underground. The longer the residence time of water in the underground, the higher the silicate concentration (e.g., Burns et al., 2003; Kendall et al., 2001; Wels et al., 1991) Since the only production of silicate in the Olewigerbach catchment is of geogenic origin, silicate concentrations may serve as a proxy of prolonged contact with the underground. Fast flow paths, rain and surface runoff might lead to comparably lower concentrations and are highly variable in time, while deep groundwater passages lead to high silicate concentrations and are more constant in contribution towards the stream flow (Stewart et al., 2007). At the monitoring locations (Figure 2b) of both reaches of the Olewigerbach catchment, shallow groundwater wells (1.5 m depth) where installed in October 2020. Two groundwater wells, the first at the riparian zone within 1.2 m to 1.5 m distance (depending on topography and soil depth) to the streambed, the second in a straight line at 3 m distance. Per reach three of these transects have been installed. Following October 2020, groundwater wells were sampled along with the stream during thirty measurement campaigns. Thus, resulting in three stream water samples as well as six groundwater samples per measurement day and reach. Hence, three silicate concentration values per layer (stream, riparian, groundwater) were taken. Samples were filtered and acidified in the laboratory at the same day. Silicate measurements (± 8%) were carried out by Atom Adsorption Spectrometry (contrAA 300). Relating reach scale variability of silicate concentrations in ground- and surface water to HT we calculated variation coefficients of silicate (var) concentrations per measurement day and reach (n= 9):

$$var_{ij} = \frac{\sigma_{ijk_{(1-9)}}}{\mu_{ijk_{(1-9)}}} \tag{8}$$

With variation coefficient of day i at reach j (var_{ij}) by standard deviation (σ_{ijk}) and mean (μ_{ijk}) of all nine silicate concentrations k (Figure 2b).

2.2.3 Characterization of drainage behavior utilizing Delayed flow separation

Baseflow dynamics can be viewed as an integrated spatial signal with multiple components (Curtis et al., 2020; Stoelzle et al., 2020). To account for variability in recession behavior, Stoelzle et al. (2020) developed the delayed flow index (DFI), which considers dynamic contributions from multiple sources during stream flow recession. The DFI is based on the smoothed minima method (Gustard et al., 1992), which involves identifying streamflow minima in consecutive periods of a block size (N). The DFI at N is then calculated as the ratio of the sum of delayed flow to the sum of the total in-stream discharge. The computation of the DFI is explained in detail in Stoelzle et al. (2020).

In this study, we carried out delayed flow separation at both reaches using hydrograph time series from August 2018 to January 2022 in 5-minute resolution, which were converted to 6-hour time steps. DFI calculation was performed using the R code available in the R package lfstat (https://CRAN.R-project.org/package=lfstat, Koffler et al., 2016). As in Stoelzle et al., (2020) the DFI covers a delay (N) from 0 to 60 days. Since both reaches are in close proximity, only variations in drainage behavior shaped through groundwater storages and their architecture should be represented in the reach-specific DFI curves. Hence, we characterized reach-specific drainage behavior by utilizing DFI analysis for both reaches.

DFI values represent the fractional amount of event water present in the stream at block N after the event itself. A steep decline in DFI towards a low percentage of event water present, represents dominant short-delayed contributors i.e., a fast drainage behavior, while the opposite represents slow drainage behavior with significant intermediate delayed contributions stabilizing at high baseline delay (Stoelzle et al., 2020). Further, we defined drainage before N=5 in the DFI curve to be quick flow (equivalent to the definition of quick flow in the IH-UK base flow separation method (Gustard et al., 1992), and all after the DFI stabilizes as very slow flow (i. e. longest lasting groundwater storage). With the part of the DFI curve in-between as the result of intermediate storage interaction. This allows for the characterization of drainage behavior and relative groundwater storage capacity in conjunction with HT-induced mixing in the stream at both reaches with contrasting features over several seasons.

3 Results

3.1 Reach Comparison and Characterization

We analyzed the Olewigerbach catchment regarding slope-valley transitions and identified two reaches with contrasting cross-sectional shapes: Selecting one reach with a steep valley cross-section (V-shape) and one with a less steep cross-section (U-shape).

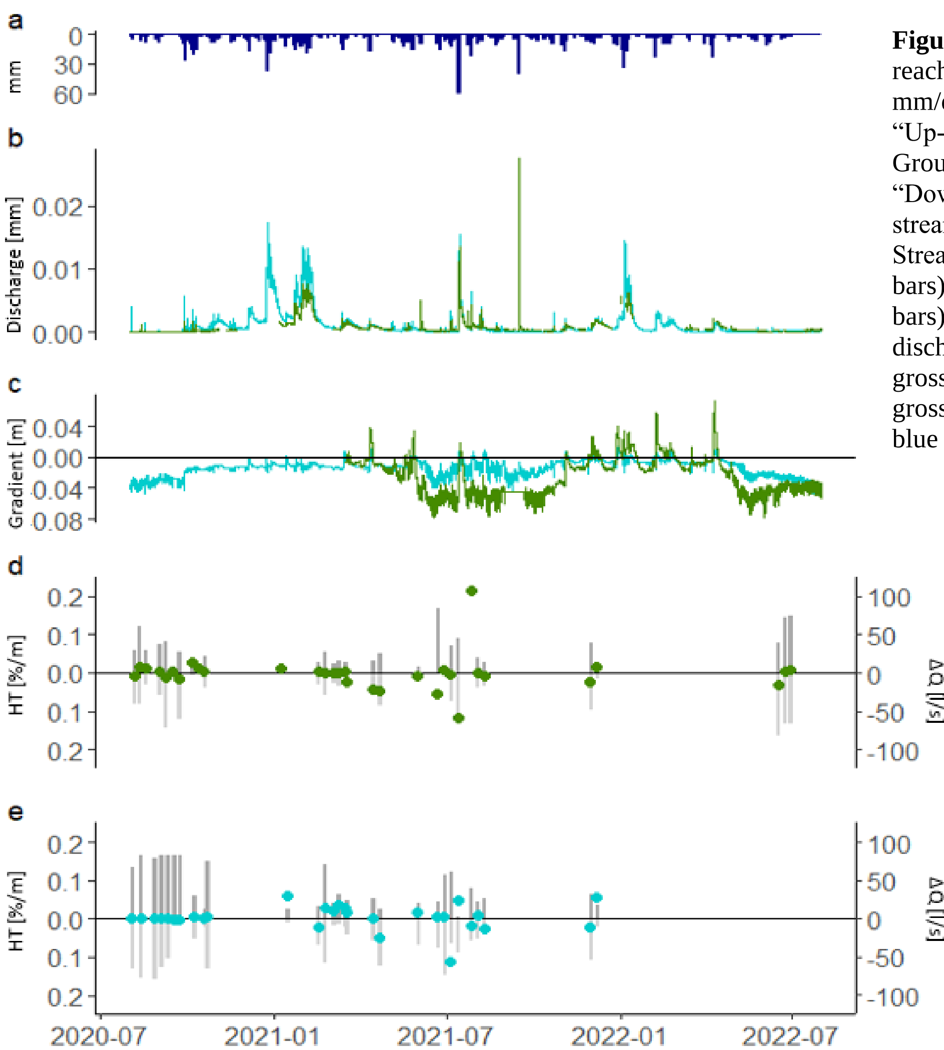

Figure 3. (**a**) Precipitation at the reach (mm). (**b**) Hydrograph in mm/d of “Down-Stream” green, “Up-stream” blue. (**c**) Groundwater Gradient in m “Down-Stream” green, “Up-stream” blue. (**d**) “Down-Stream” gross Loss (light grey bars) and gross Gain (dark grey bars) in l/s, green dots net discharge in l/s. (**e**) “Up-Stream” gross Loss (light grey bars) and gross Gain (dark grey bars) in l/s, blue dots net discharge in l/s.

Comparing the reach valley structure, the "Up-Stream" reach is narrow and steep, and the "Down-Stream" reach presents itself as flatter and wider (Figure 4a). Both reaches receive approximately the same amount of rainfall over the year (Figure 3a), with precipitation derived by the areal weighted mean of three, near catchment weather stations (Oberzerf; 43/VOZ [49.58922, 6.67506], Trier-Irsch; 230/VIR [49.72599, 6.69570], Trier-Petrisberg; [49.7478, 6.6581]; Deutscher Wetterdienst). The "Up-Stream" reach reacts fast with areal peak runoff exceeding the "Down-Stream" reach during flood peaks. The near stream groundwater gradients of both reaches are mostly constant negative over the observation period, only in conjunction with rain events gradients change direction, briefly (Figure 3c). The seasonal oscillation of the hydraulic gradients is more pronounced at the "Down-Stream" reach. Expressing, Q_{Loss} and Q_{Gain} as a fractional loss or gain per unit distance (m) reveals, that at the "Up-Stream" reach a larger fraction of discharge is subject to HT most of the time, especially under summer low flow conditions. For most HT measurements (Figure 3e & d) net discharge changes where exceeded. Further, the reach specific DFI curves provide an intense contrast, with the "Up-Stream" reach draining 75% of its initial input after the first five days as quick flow (Nathan & McMahon, 1990), while the "Down-stream" reach only drains 50% (Figure 4b). The larger quick flow component of the "Up-Stream" reach fits well with the steeper valley cross-section and the less delayed hydrograph response to rain events.

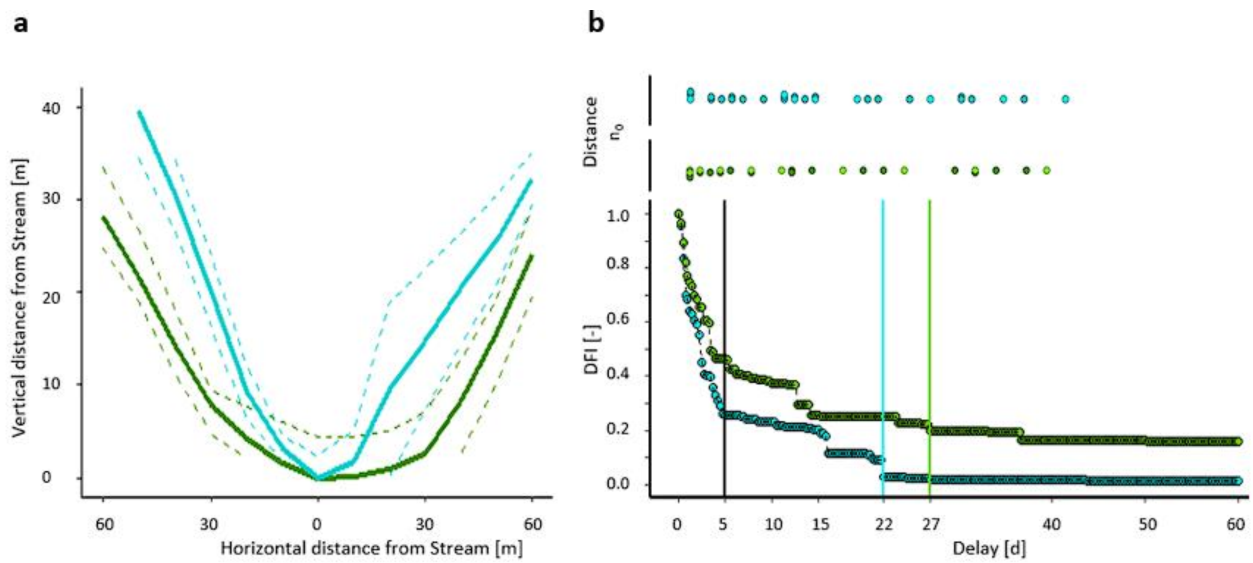

Figure 4. (**a)** Mean valley cross-section profiles and standard deviations of "Down-Stream" (green) and "Up-stream" (blue). (**b**) Reach specific delayed flow curves (DFI). DFI representing the contribution of event water to stream flow over time. "Down-Stream" green, "Up-stream" blue. Quick-flow>5 days delay (black vertical line, entering storage sustained stream flow after 22 days delay (Up-Stream, blue) and after 27 days delay (Down-Stream, green).

The wider valley cross-section at the "Down-Stream" reach with a dampened hydrograph response to rain events is apparent in the lower quick flow component of its DFI curve (Figure 4b). Characterizing the "Up-Stream" with the DFI curve suggests a much faster drainage of the associated catchment with a large quick flow component, a short intermediate flow and only 3% contribution to baseflow after 22 days. The "Down-Stream" reach shows a prolonged intermittent flow and a baseflow contribution of 20% after 27 days, thus presenting slower drainage behavior.

3.2 Hydrological Turnover and Silicate Variability

Comparing the overall results of the HT measurements, the "Down-Stream" reach shows an average discharge of 132 l/s on measurement days with an average net Q change of -0.7 l/s, and an average gross loss of 34 l/s (max: 193 l/s; min: 0.5 l/s) and gross gain of 29 l/s (max: 135 l/s; min: 2.5 l/s).

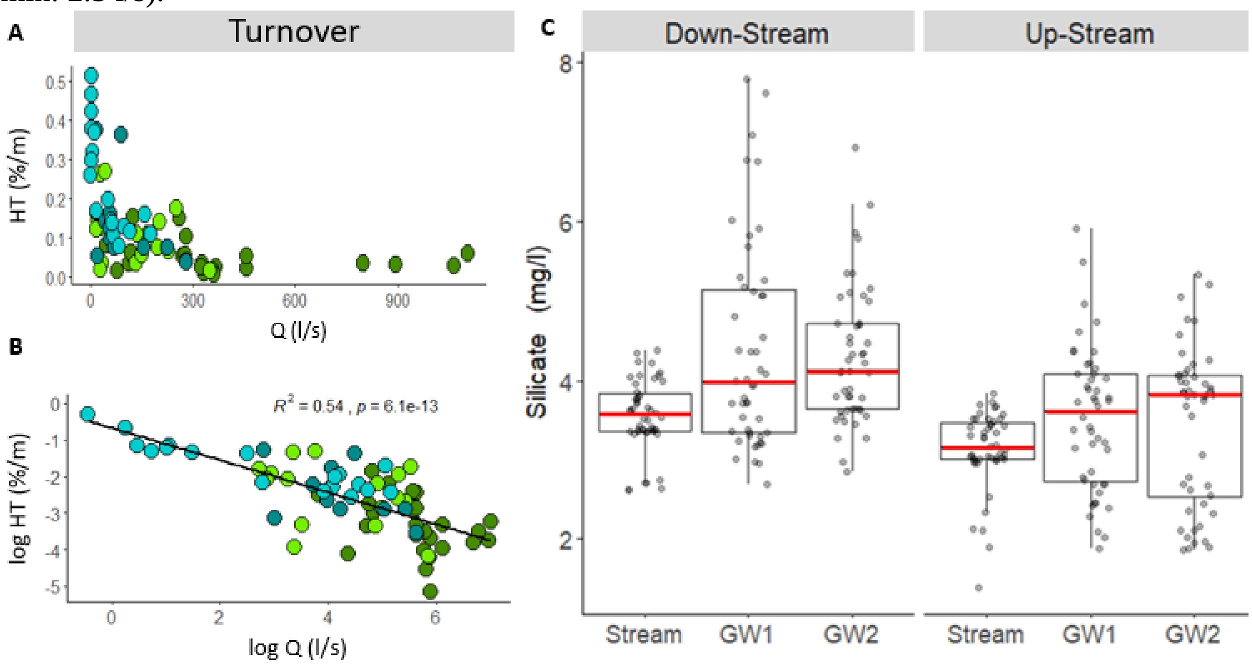

Figure 5. (**a**) "Down-Stream" (green) and "Up-Stream" (blue) reaches, with HT as fraction of discharge per meter compared to discharge (l/s). (**b**) log HT as fraction of discharge per meter and log Q in liter per seconds with linear regression, "Down-Stream" n= 44, "Up-stream" n= 29. (**c**) Boxplots of Silicate concentrations at sampling positions (mg/l) at both reaches "Down-Stream" (n=42) and "Up-Stream" (n=48), red line indicating the median.

The "Up-Stream" reach shows average discharge of 66 l/s with an average net Q change of 1.7 l/s, and an average gross loss of 17.5 l/s (max: 60 l/s; min: 1.5 l/s) and gross gain of 22 l/s (max: 113 l/s; min: 0.6 l/s). We found for both reaches a significant regression of the log HT (%/m) and discharge (Figure 5b). However, reaches differ in strength of correlation (Figure 6). Examining HT in the context of discharge reveals that there are distinct differences between the reaches: At the study sites the average magnitude of discharge changes with season, with low flows in summer and high flows in winter. The apparent potential relation between discharge and HT sets the condition of seasonal HT patterns. However, such seasonality is presented in different strength reach wise. With the upstream reach showing larger differences in fractional HT in summer compared to winter (Figure 5b). At the downstream reach Q net| was neither correlated with Q, nor with HT or the hydraulic gradients (Figure 6). In contrast to that the "Up-Stream" reach presents all-over significant correlations of HT to all other parameters except silicate variability (Figure 6). Thus, the "Down-Stream reach presenting it-self more independent in its HT processes from apparent discharge conditions. HT changes with groundwater gradient, however there is no pattern to observe regarding net changes in stream flow and groundwater gradients at both reaches (Figure 6). The sampled silicate concentrations at the reaches show a general increase from the stream towards the second groundwater well (Figure 5c). Silicate concentration as a proxy for underground contact shows throughout the stream samples and groundwater samples generally higher median concentrations at the faster draining "Up-Stream" reach compared to the

"Downstream" reach. However, the variability in the middle groundwater wells (GW1) appears to be very high (Figure 5c). The applied analysis of the silicate concentration utilizes this large variability in the form of variation coefficients (eq. 8), analyzed in conjunction with all other reach parameters (Figure 6). In the case of Q net, as a conservative measure of exchange with the underground (e.g., Szeftel et al., 2011; Ruehl et al., 2006) silicate variation coefficients do not significantly correlate. Hence, net exchange does not produce a signal of mixing within the silicate tracer variation of the qua groundwater sampling defined boundary layer between ground- and surface water. We observe that mixing in the form of silicate tracer variability exclusively in conjunction with HT at the "Down-Stream" reach (Figure 6). At the "Down-Stream" reach silicate variability shows a strong relation to HT as well as gross loss hinting towards "turnover induced" mixing between Stream and groundwater storages. At the "Up-Stream", in summer no HT silica variation relation is to be observed only in winter with $p = 0.026$ (log QLoss/varSi, $R^2 = 0.59$) and $p = 0.027$ (log HT/silicate variation, $R^2 = 0.59$). In summer, variation coefficients are present in a compressed range compared to winter with a narrow HT range at the "Up-Stream" reach as well. That smaller range in variation and in HT reflects that summer and winter states of the "Up-Stream" reach system are functioning seasonally different with respect to GW-SW interaction and its associated mixing within the bidirectional flow patterns. Since, silicate samples where only taken 13-15 times and logging of the groundwater gradient started not until spring 2021, the data base is not sufficient to analyse silicate variation in the context of groundwater gradients in a comparative manner for the reaches.

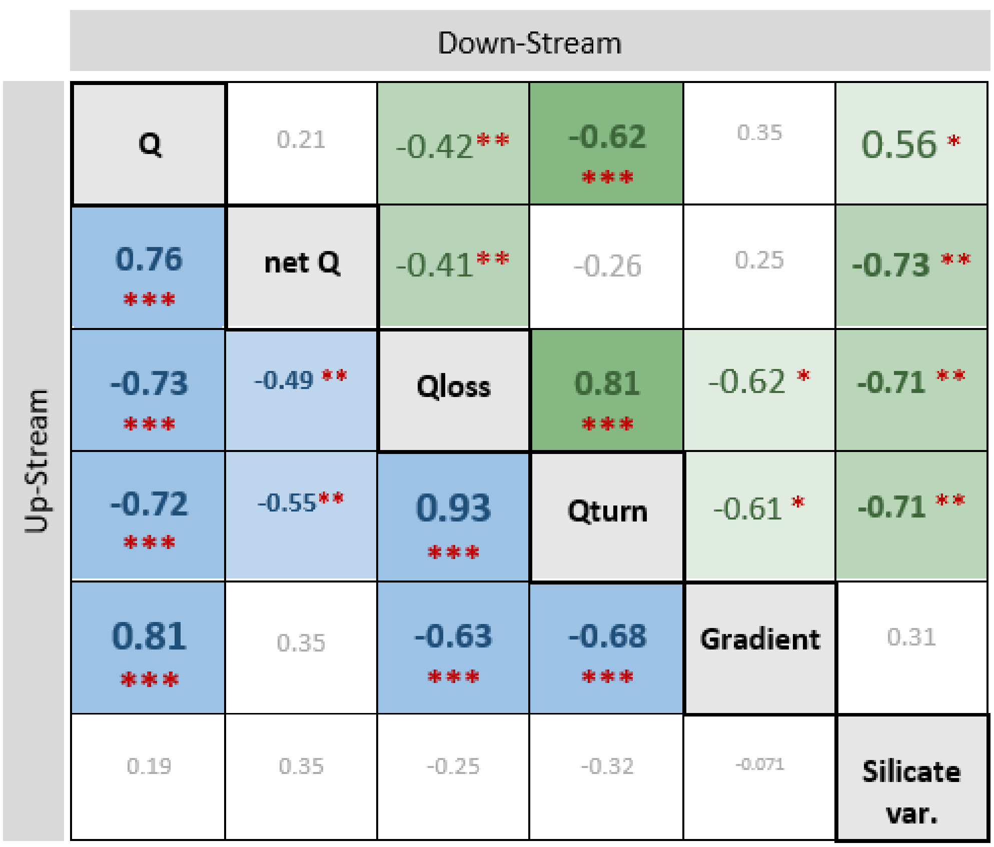

Figure 6. Correlation matrixes of the "Down-Stream" (green) and "Up-Stream" (blue) reach, (log) Q in l/s, n=29(Up-Stream)/46(Down-Stream), (log) netQ change in l/s, n=29/43, (log) Q_{Loss} in %/m, n=29/43, (log) Q_{Turn} %/m, n=29/43, Groundwater Gradient in m n=29/15 and silicate variation, n=15/13. Spearman's Rho, red stars indicating significance.

3.3 Inner Reach Turnover Variability

The experimental setup of this study (Figure 2) logs three BTCs per tracer test, HT of two sub segments of each reach and HT of the total reach can be compared (compare Figure 2, A; B; C). Thus, allowing for the analysis of reach specific spatial turnover variability.

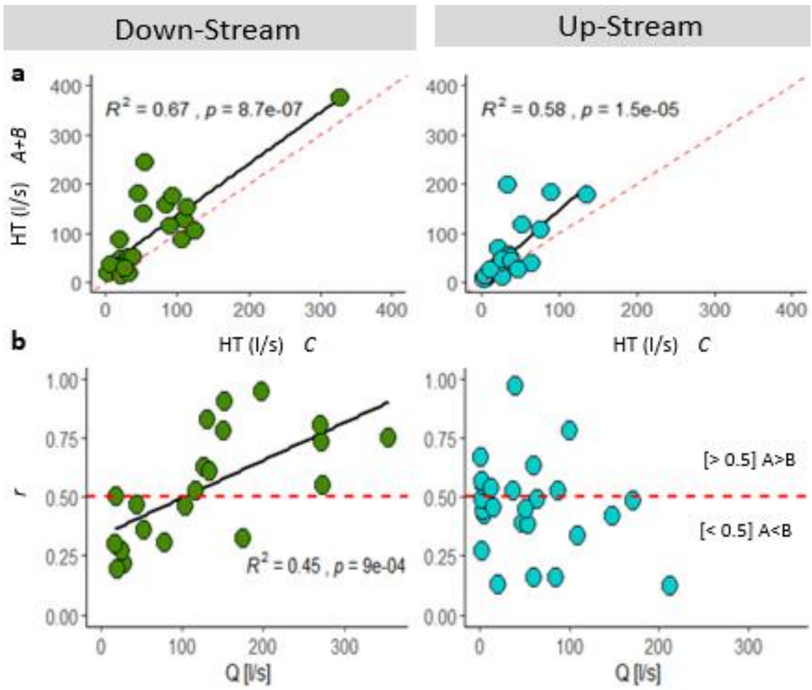

Figure 7. (**a**) Comparison of the cumulative HT of both sub-reach sections (HT A+B), with each section = 250m and the total reach (HT C) = 500m. Red dotted line as 1:1-line. HT displayed in l/s." Down-Stream" reach green, "Up-Stream" reach blue. (**a**) Comparison of discharge to sub-reach contribution to HT as ratio r (eq. 7). Red dotted line marking equal HT contribution of both sub-reaches. "Down-Stream" reach green, "Up-Stream" reach blue.

In contrast to the simple initial assumption, that the sum of sub-reach bidirectional flows equals to the total reach flows it is shown that the sum of sub-reaches HT is in most of all cases exceeding the total reach HT estimation (Figure 7). HT quantification (eqs. 3 to 5) is a function of tracer mass loss, the mass recovery of the total reaches is exceeding the recovery of the sub-reaches. Shorter reach lengths overestimate HT, systematically, especially at higher HT magnitudes (1:1 line Figure 7a). Ratios r of relative sub-reach contribution (eq. 7) to overall HT at each reach, reveal distinct differences between both reaches. Sub-reach contributions are highly variable over time. At the "Down-Stream" reach, *r* is changing with apparent discharges (Figure 7b). Thus, identifying that the reach is susceptible to flow conditions in its spatial HT contribution. With the first sub-reach contributing more towards overall HT during low flow conditions, transferring with higher discharges to the second sub-reach being dominant in HT its contribution. At the "up-stream" reach there is no such behavior observable (Figure 7).

4 Discussion

Temporal and spatial variability in streamflow contributions can change over time, influenced by hydrological factors (Ward et al., 2019). In this study, we compared two reaches within the Olewigerbach catchment. These reaches display distinct geomorphological settings, evident in their valley cross-section profiles (Figure 4), leading to contrasting hydrological conditions. HT magnitudes can vary across short distances (Jimenez-Fernandez et al., 2022). To address this, we designed the experimental setup for both total reach and sub-reach HT estimations (Figure 2).

4.1 Reach Comparison

4.1.1 HT Discharge Relationship

Previous research (e.g., Covino et al., 2011; Mallard et al., 2014) states that apparent streamflow magnitudes explain the part of apparent discharge subject to HT well. In the works of Covino et al. (2011) and Mallard et al. (2014), HT measurements took place between May and September. In other studies, HT measurements were carried out in one catchment during summer baseflow recession (Payn et al., 2009), in four sets under baseflow conditions (Ward et al., 2013), in two short campaigns at baseflow conditions in summer and winter (Jimenez-Fernandez et al., 2022), or in seven campaigns at different streams over one hydrological year (Jäkhel et al., 2022). We present a dataset where all these periods are covered by measurements during two hydrological years. Thus, we captured most of the expected variability in HT throughout a year (Figure 6). The empirical equation presented by Mallard et al. (2014), based on discharge magnitudes and drainage area, may not apply for catchments with such a strong variance in valley shape and drainage behaviour variability as presented in this study. We show that the "Up-Stream" reach can be defined as a comparatively fast-draining reach (Figure 4), where an empirical equation based on discharge magnitudes yields robust results with respect to HT prediction, especially under low flow summer conditions (Figure 5). Therefore, we suggest that such an approach is beneficial for catchments with homogeneous fast drainage behaviour. Also, seasonality is an important factor, with generally larger magnitudes of discharge in the winter season compared to summer seasons (European Atlantic climate). We suggest the necessity, of accounting for the possible shift in spatial HT contribution with discharge and along the stream network as well.

4.1.2 Silicate as a Geogenic Tracer for HT Processes

The mass balance-based slug tracer injection, in combination with discharge quantification by dilution gauging, is currently the only method for quantifying HT. In the research of Ward et al. (2013), HT measurements coupled with momentum analysis were applied to distinguish between long- and short-term storage of gross losses of a reach. Long-term gross losses suggest potential groundwater recharge, indicating that the window of detection is crucial in differentiating between long- and short-term storage of streamflow. Therefore, the general question arises of how to observe HT independently of tracer breakthrough curves. With the goal to confirm, that the quantification of HT is not an accumulation of method inherent variability in tracer recovery in the window of detection, we chose to observe silicate concentration in near-stream groundwater wells (Figure 2). First to confirm that HT-induced bidirectional movement of water masses is connected to HT and second, that there is HT-induced mixing between groundwater and surface water. Thus, affecting in turn solute concentrations within the stream as well as in the boundary layer towards the groundwater, covering what is referred to as the riparian zone and/or the hyporheic zone (e.g. Wondzell et al., 2011; Ward et al., 2013; 2019).Considering silicate concentration in groundwater and surface water strictly as a product of residence time in the underground (e.g. Burns et al., 2003; Kendall et al., 2001; Wels et al., 1991), its variation coefficients visualize HT-induced mixing between stream water and storages with different drainage velocities (Figure 4 & 6). Under the assumption of slower flow velocities in the hyporheic zone, as well as in the connected groundwater storages, there is a severe memory effect of silicate concentrations between the stream and its surroundings. Thus, only the analysis of relative silicate concentrations between the stream and groundwater across the reach yielded insightful results in the form of variation coefficients. Under the hypothesis of HT affecting the area of silicate sampling, we associate a decline in silicate variation with a high fraction of discharge subject to turnover, leading to mixing of ground and surface water in the defined area. On the other hand, high variation implies less connectivity and mixing through HT. We found that this behaviour can be clearly observed at the "Down-stream" reach, where HT correlates with silicate variation throughout the year (Figure 6). However, such approach relies on detectable differences in silicate concentrations of the mixing members as well as the abundance of multiple of such mixing members.

4.1.3 Seasonality

Analysing reach-specific DFI curves, we deduce that the faster-draining "Up-Stream" segment has shorter transit times and limited storage compared to the slower-draining "Down-Stream" area, a pattern evident in the higher median silicate concentrations. However, the relationship between silicate variability in the boundary layer between ground and surface water is only observable at the slower-draining reach. We present a conceptual model, visualizing the interplay of storage states and drainage behaviour, rooted in topography shaping seasonality of HT at both reaches at the Olewigerbach (Figure 8). There is a seasonal shift at the fast-draining reach with lower storage capacity from predominantly GW-SW interaction as an exchange towards streamflow recycling, as described by Covino et al. (2011), where each unit of the stream network has an increasing chance of receiving formerly lost stream flow in the process of HT multiple times.

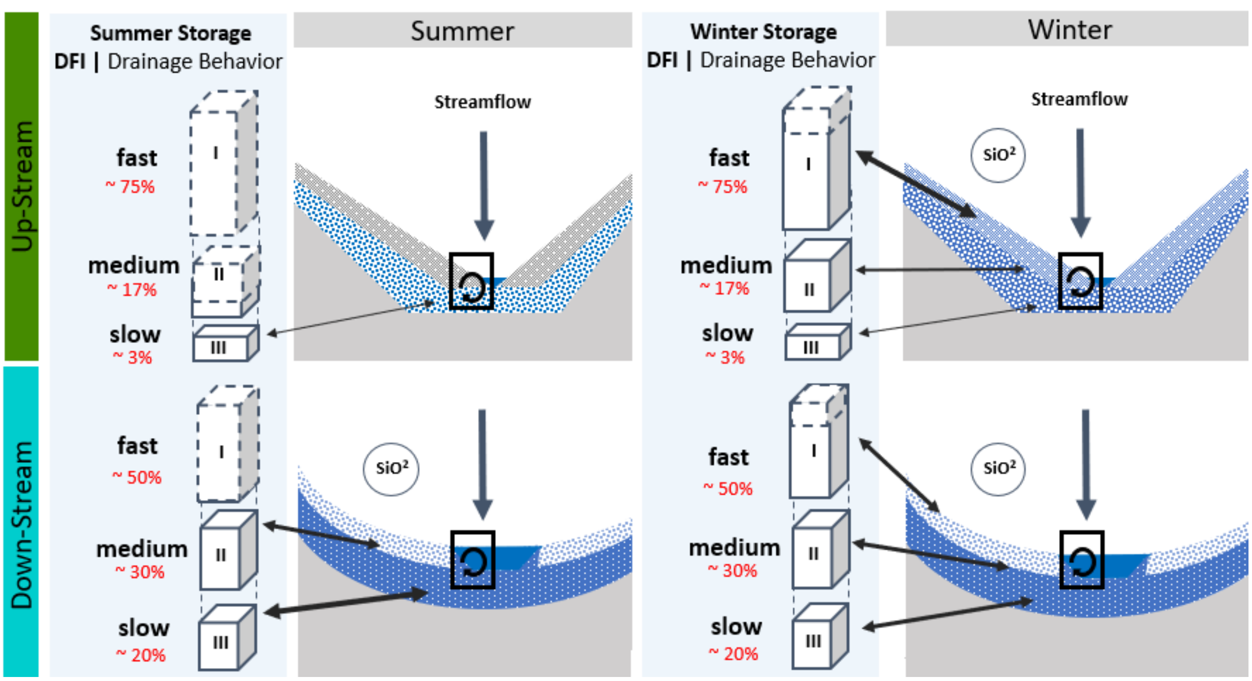

Figure 8. Concept of seasonal differences in dynamic storage contribution in HT induced mixing at the “Up-Stream” (upper panels) and “Down-Stream” (lower panels) reaches. With fast (I), medium (II) and slow (III) dynamic storages and their storage state during summer and winter, the area of HT interaction (black box) and indication of HT correlation with silicate variation coefficients (grey circle).

A possible shift from groundwater-born gross gains towards a dominant recycling of former stream flow, mostly in exchange with the hyporheic zone, is supported by the statement of Zimmer et al. (2016), that streams can temporally act as both, sources and sinks for groundwater and run-off can be produced at low storage states, independent of deep groundwater contributions. We found that this might be the case for the headwater of the Olewigerbach. Stream flow is sustaining itself across sections with limited access to groundwater storages. This is apparent in the "Up-Stream" reach silicate concentrations during summer, where no correlation to HT was observed (Figure 6 & 8), indicating insufficient gradients between silicate concentrations of the contributing mixing members. However, at the “Up-Stream” reach during summer groundwater influx in volume as well as in silicate concentration difference towards the apparent streamflow from the head of the stream is no longer capable producing a HT signal of mixing between storages and the stream (Figure 8). Hence, HT may consist predominantly of recycled streamflow. Only during winter, when storages at the "Up-Stream" reach are sustainably full, the effect of turnover is visible within the silicate variation relation ($R^2= 0.59; n=8; p=0.027$). At the "Down-Stream" reach, we do not observe this seasonality. Here, the storage contribution is sustainable throughout the year, as supported by the information of the reach DFI curve (Fig 4 & 8).

4.2 Inner Reach Variability

According to the conceptual stream channel profile proposed by Payn et al. (2009), multiple flow paths do contribute when measuring HT using the tracer-based method. Shorter reaches, examined for HT, have a higher probability of short-term storages or delay of stream flow marked by tracer, resulting in marked water in transient storage that may not enter the stream again within the detection window or bypass the detector entirely (Payn et al., 2009; Ward et al., 2013). In consequence, HT may overestimate increasingly at shorter reaches. However, our results (Figure 7) demonstrate that this overestimation is systematic across different discharge magnitudes and might be reach-specific. Regarding sub-reach contribution over time and discharge magnitudes, we observe contrasting behaviour of the two sampled reaches, with the "Down-stream" reach changing in spatial HT contribution with discharge, while the "Up-stream" reach does not, showing a systematic change. The difference in valley shape may produce flow pathway activation dependent on discharge at the "Down-stream" reach, resulting in a shift in spatial streamflow contribution and thus an increase of HT at these areas.

4.3 Controls of HT variability and implications for solute transport

HT, moving beyond the scope of analysing mere net exchange in GW-SW interaction, emphasizes the impact of total gross exchange (Covino & McGlynn, 2007), encompassing all interactions of moving water with its environment. This includes the constant replacement of some portion of the water volume and the reintroduction of former exfiltrate water volume, as well as the introduction of additional "fresh" groundwater. The question of what fraction of the gross gain is recycled in the stream flow from the headwaters and what is on-site groundwater influx must be considered from a Lagrangian and Eulerian perspective on HT processes, as suggested in Payn et al. (2009), applied in Covino et al. (2011), and continued in Mallard et al. (2014). Our findings indicate that the fractional makeup of these observed HT processes varies across time and space. Additionally, as the autonomous exchange capacity with the external medium (groundwater storage connectivity) diminishes, the moving volume itself gains prominence as a pivotal parameter in influencing exchange within the reference frame cells. As recycled water within the HT process gains prevalence, it reinforces the HT discharge relationship, and conversely (Figure 5 & 8). Certain properties promote exchange with the hyporheic zone. Sediment permeability and stream velocity are important parameters in hyporheic exchange (Packman & Salehin, 2003). In summer, at the fast-draining "Up-Stream" reach, we observe HT rates up to 90% of initial streamflow exchanged while storage contribution is expected to be low. In addition to that, our findings promote that the reach-specific drainage behaviour influences the seasonality of HT, and the fast-draining reach coincides with an overall dampened seasonal oscillation of the groundwater gradient (Figure 2a), together with limited activation of additional flow paths, resulting in no significant change of spatial HT contribution (Figure 2b). Therefore, this reach engages in HT as streamflow recycling to a large degree, especially in summer. However, in winter, the silicate HT relation suggests a shift in the dominance of forcings shaping HT composition towards interaction with groundwater storages. Thus, HT is important in GW-SW interaction under sufficient storage state (Figure 8). At the "Down-Stream" reach, the silicate HT relation is constant over the year. Here, onsite groundwater appears to be dominant, even though the probability of streamflow recycling with distance from the headwaters is increased (Covino et al., 2011). Thus, the HT-induced mixing constantly affects the near-stream sphere of GW-SW interaction, illustrating the potential for bidirectional lateral solute transport as well as transport from the headwaters at the "Down-Stream" reach throughout the year, while bidirectional lateral solute transport at the "Up-Stream" is seasonal.

5 Conclusion

The data set compiled within this study, spanning two hydrological years, enabled us to capture the variability of HT throughout the year for two contrasting sites within one catchment. As stated in prior research (e. g. Covino et al., 2011; Mallard et al., 2014), we could establish site specific negative correlations between stream flow and HT. In contrast, absolute changes in stream flow on the reach scale were not correlated with local hydraulic gradients.

Through the comparison of two geomorphologically contrasting reaches, we could show that a larger alluvial groundwater storage supports local stream flow sustainability and decouples HT from absolute changes in stream flow, while smaller groundwater storages and faster drainage behavior could be negatively correlated with absolute stream flow changes on the reach scale.

This is further supported by the assessment of silicate variability between the stream and the near-stream groundwater, where we could show that in-reach silicate variation increases significantly with the decrease of HT under groundwater dominated flow conditions. This is especially apparent in the seasonal shift of the correlation between HT and silicate at the fast-draining up-stream reach, while at the down –stream reach with a slower drainage behavior and thus more stable groundwater storage state this correlation is constantly apparent throughout the year. Thereby, we demonstrate that the use of near stream groundwater silicate variability can serve as a valuable proxy revealing the decoupling of ground and surface water, by indicating a shift in HT from groundwater dominated exchange fluxes to a dominance of stream flow recycling. At the reach level, we found that spatial contributions to HT can vary over time, and we observed systematic underestimation of HT with a decrease of reach length at both reaches of the Olewigerbach catchment.

Our findings highlight the intricate balance between connectivity and storage state influenced by reach drainage behavior and thus shaping the seasonality of HT. The seasonal condition of groundwater storages at a stream reach may control the mix of HT and the relative contribution of groundwater in that process. The observed HT variability presents itself as a driving force in the mixing of physically different water masses, presenting itself clearly, even in a small catchment between two different reaches.

For the future development of hydrological catchment models this study might provide a new perspective on which drivers might be helpful for implementing HT into catchment models successfully.

Acknowledgments

The Authors thank Sven Ulrich for his help during the data acquisition and Beate Krämer for her help with the Silicate analysis in the lab. The author Lars Bäthke is funded by a PhD-stipend of the Studienwerk Villigst e. V., Germany.

Open Research

Data is available at https://doi.org/10.5281/zenodo.8321159

References

Arnon, S., Marx, L. P., Searcy, K. E. & Packman, A. I. (2010), Effects of overlying velocity, particle size, and biofilm growth on stream–subsurface exchange of particles. *Hydrological Processes*, *24*(1), 108–114.

Arnon, S., Yanuka, K. & Nejidat, A. (2013). Impact of overlying water velocity on ammonium uptake by benthic biofilms. *Hydrological Processes*, *27*(4), 570–578.

Banzhaf, S. & Scheytt, T. (2009), Auswirkung einer künstlichen Hochwasserwelle auf den fließgewässernahen Grundwasserleiter. *Grundwasser*, *14*(4), 265–275. doi:10.1007/s00767-009-0109-x

Battin, T. J., Kaplan, L. A., Findlay, S., Hopkinson, C. S., Marti, E., Packman, A. I. & Sabater, F. (2008), Biophysical controls on organic carbon fluxes in fluvial networks. *Nature geoscience*, *1*(2), 95–100.

Battin, T. J., Besemer, K., Bengtsson, M. M., Romani, A. M. & Packmann, A. I. (2016), The ecology and biogeochemistry of stream biofilms. *Nature Reviews Microbiology*, *14*(4), 251–263.

Bencala K. E. (2000). Hyporheic zone hydrological processes. *Hydrological Processes*, *14*, 2797–8.

Bencala K. E. & Walters, R. A. (1983), Simulation of solute transport in a mountain pool-and-riffle stream: a transient storage model. *Water Resources Research*, *19*(3):718–24.

Bergstrom, A., Jencso, K. & McGlynn, B. (2016), Spatiotemporal processes that contribute to hydrologic exchange between hillslopes, valley bottoms, and streams, *Water Resources Research*, *52*, 4628–4645. doi:10.1002/2015WR017972

Blumstock, M., Tetzlaff, D., Malcolm, I., Nuetzmann, G. & Soulsby, C. (2015), Baseflow dynamics: Multi-tracer surveys to assess variable groundwater contributions to montane streams under low flows. *Journal of Hydrology*, *527*, 1021–1033. doi: 10.1016/j.jhydrol.2015.05.019

Burns, D. A., Plummer, L. N., McDonnell, J. J., Busenberg, E., Casile, C., Kendall, C., Hooper, R. P., Freer, J.E., Peters, N. E., Beven, K., Schlosser, P. (2003), The geochemical evolution of riparian ground water in a forested piedmont catchment. *Groundwater*, *41*(7): 913–925.

Cardenas, A. A., Amin, S. & Sastry, S. (2008), Secure control: Towards survivable cyber-physical systems. In 2008 The 28th International Conference on Distributed Computing Systems Workshops, 495–500. IEEE.

Cirpka, O. A., Fienen, M. N., Hofer, M., Hoehn, E., Tessarini, A., Kipfer, R. & Kitanidis, P. K. (2007), Analyzing bank filtration by deconvoluting time series of electric conductivity. *Groundwater*, *45*(3), 318–328.

Covino, T., McGlynn, B. & Mallard, J. (2011), Stream-groundwater exchange and hydrologic turnover at the network scale. *Water Resources Research*, *47*(12), doi:10.1029/2011WR010942

Covino, T. & McGlynn, B. L. (2007), Stream gains and losses across a mountain-to-valley transition: Impacts on watershed hydrology and stream water chemistry. *Water Resources Research*, *43*(10). doi:10.1029/2006wr005544

Curtis, J. A., Burns, E. R. & Sando, R. (2020), Regional patterns in hydrologic response, a new three-component metric for hydrograph analysis and implications for ecohydrology, Northwest Volcanic Aquifer Study Area, USA. *Journal of Hydrology: Regional Studies*, *30*, doi:100698

Day, T. J. (1976), On the precision of salt dilution gauging. *Journal of Hydrology*, *31*(3), 293–306. doi:10.1016/0022-1694(76)90130-X

De Falco, N., Boano, F., Bogler, A., Bar-Zeev, E. & Arnon, S. (2018), Influence of stream-subsurface exchange flux and bacterial biofilms on oxygen consumption under nutrientrich conditions. *Journal of Geophysical Research: Biogeosciences*, *123*, 2021–2034. doi:10.1029/ 2017JG004372

Dudley-Southern, M. & Binley, A (2015), Temporal responses of groundwater-surface water exchange to successive storm events, *Water Resources Research*, *51*, 1112–1126, doi:10.1002/2014WR016623

Gustard, A., Bullock, A. & Dixon, J. M. (1992), Low flow estimation in the United Kingdom, Institute of Hydrology, Wallingford, UK, 108, 88.

Gücker, B. & Böchat, I. G. (2004), Stream morphology controls ammonium retention in tropical headwaters. *Ecology 85*, 2818–2827.

Harvey, J. W. & Bencala, K. E. (1993), The effect of streambed topography on surface-subsurface water exchange in mountain catchments. *Water Resources Research*, *29*(1), 89–98.

Harvey, J. W., Wagner, B. J. & Bencala, K. E. (1996), Evaluating the reliability of the stream tracer approach to characterize stream-subsurface water exchange. *Water Resources Research*, *32*(8), 2441–2451. doi:10.1029/96WR01268

Jähkel, A., Graeber, D., Fleckenstein, J. H. & Schmidt, C. (2022), Hydrologic turnover matters - Gross gains and losses of six first-order streams across contrasting landscapes and flow regimes. *Water Resources Research*, *58*, e2022WR032129. doi:10.1029/2022WR032129

Jimenez-Fernandez, O., Schwientek, M., Osenbrück, K., Glaser, C., Schmidt, C. & Fleckenstein, J. H. (2022), Groundwater-surface water exchange as key control for instream and groundwater nitrate concentrations along a first-order agricultural stream. *Hydrological Processes*, *36(2), e14507*. doi:10.1002/hyp.14507

Kalbus, E., Reinstorf, F. & Schirmer, M. (2006), Measuring methods for groundwater–surface water interactions: a review. *Hydrology and Earth System Sciences*, *10*(6), 873–887.

Kendall, C., McDonnell, J. J., & Gu, W. (2001), A look inside 'black box' hydrograph separation models: a study at the Hydrohill catchment. *Hydrological Processes*, *15*(10), 1877–1902.

Kilpatrick, F. A. & Cobb, E. D. (1985), Measurement of discharge using tracers. U.S. Geological Survey Techniques of Water-Resources Investigations.

Klaus, J. & McDonnell, J. J. (2013), Hydrograph separation using stable isotopes: Review and evaluation. *Journal of Hydrology*, *505*, 47–64. doi: 10.1016/j.jhydrol.2013.09.006

Krein, A. & Schorer, M. (2000), Road runoff pollution by polycyclic aromatic hydrocarbons and its contribution to river sediments. *Water Research*, *34*(16), 41104115. doi:10.1016/S0043-1354(00)00156-1

Krein, A., Symader, W. (2000), Pollutant sources and transport patterns during natural and artificial flood events in the Olewigerbach and Kartelbornsbach basins, Germany. IAHS Publikation, *263*, 167–173.

Krein, A. & De Sutter, R. (2001), Use of artificial flood events to demonstrate the invalidity of simple mixing models. *Hydrological Sciences Journal*, *46*(4), 611–622.

Mallard, J., McGlynn, B. & Covino, T. (2014), Lateral inflows, stream-groundwater exchange, and network geometry influence stream water composition, *Water Resources Research*, *50*, 4603–4623, doi:10.1002/ 2013WR014944

Malzone, J. M., Anseeuw, S. K., Lowry, C. S. & Allen-King, R. (2016), Temporal Hyporheic Zone Response to Water Table Fluctuations. *Groundwater*, *54*, 274–285. doi: 10.1111/gwat.12352

McGlynn, B. L. & Seibert, J. (2003), Distributed assessment of contributing area and riparian buffering along stream networks, *Water Resources Research*, *39*(4), 1082, doi:10.1029/2002WR001521.

McGuire, K. J., McDonnell, J. J., Weiler, M., Kendall, C., McGlynn, B. L., Welker, J. M. & Seibert, J. (2005), The role of topography on catchment-scale water residence time. *Water Resources Research*, *41*(5).

Nathan, R. J. & McMahon, T. A. (1990), Evaluation of automated techniques for base flow and recession analysis. *Water Resources Research*, *26*(7), 1465–1473.

Packman, A. I. & Salehin, M. (2003), Relative roles of stream flow and sedimentary conditions in controlling hyporheic exchange. *Hydrobiologia*, *494*, 291–297.

Payn, R. A., Gooseff, M. N., McGlynn, B. L., Bencala, K. E. & Wondzell, S. M. (2009), Channel water balance and exchange with subsurface flow along a mountain headwater stream in Montana, United States. *Water Resources Research*, *45*(11), doi:10.1029/2008WR007644

Payn, R. A., Gooseff, M., McGlynn, B., Bencala, K. E. & Wondzell, S. M. (2012), Exploring changes in the spatial distribution of stream baseflow generation during a seasonal recession. *Water Resources Research*, *48*(4), doi:10.1029/2011WR011552

Penna, D., van Meerveld, H. J., Oliviero, O., Zuecco, G., Assendelft, R. S., Dalla Fontana, G. & Borga, M. (2015), Seasonal changes in runoff generation in a small forested mountain catchment. *Hydrological Processes*, *29*(8), 2027–2042.

Ruehl, C., Fisher, A. T., Hatch, C., Los Huertos, M., Stemler, G. & Shennan, C. (2006), Differential gauging and tracer tests resolve seepage fluxes in a strongly-losing stream. *Journal of Hydrology*, *330*(1-2), 235–248.

Runkel, R. L. (1998), One dimensional transport with inflow and storage (OTIS): a solute transport model for streams and rivers. US Geological Survey Water-Resources Investigation Report, US Geological Survey, Denver, Colorado, 98–4018.

Runkel, R. L. (2002), A new metric for determining the importance of transient storage. *Journal of the North American Benthological Society*, *21*(4), 529–543.

Schmadel, N. M., Ward, A. S. & Wondzell, S. M. (2017), Hydrologic controls on hyporheic exchange in a headwater mountain stream, *Water Resources Research*, *53*, 6260–6278. doi:10.1002/2017WR020576

Schmidt, C., Bayer-Raich, M. & Schirmer, M. (2006), Characterization of spatial heterogeneity of groundwater-stream water interactions using multiple depth streambed temperature measurements at the reach scale. *Hydrology and Earth System Sciences*, *10*(6), 849–859.

Schmitgen, L. M., Bierl, R. & Schuetz, T. (2021), Model choice impacts the quantification of seasonal hyporheic exchange depths and fluxes. *Water Resources Research*, *57*(12), doi: e2021WR030298.

Schuetz, T., Gascuel-Odoux, C., Durand, P., & Weiler, M. (2016), Nitrate sinks and sources as controls of spatio-temporal water quality dynamics in an agricultural headwater catchment, *Hydrology and Earth System Sciences*, *20*, 843–857. doi: 10.5194/hess-20-843-2016

Schuetz, T. & Weiler, M. (2011), Quantification of localized groundwater inflow into streams using ground-based infrared thermography, *Geophysical. Research Letters*, *38*, L03401, doi:10.1029/2010gl046198

Staudinger, M., Stoelzle, M., Cochand, F., Seibert, J., Weiler, M. & Hunkeler, D. (2019), Your work is my boundary Challenges and approaches for a closer collaboration between hydrologists and hydrogeologists. *Journal of Hydrology*, *571*, 235–243.

Staudinger, M., Seibert, J., & van Meerveld, H. J. (2021), Representation of Bi-Directional Fluxes Between Groundwater and Surface Water in a Bucket-Type Hydrological Model. *Water Resources Research*, *57*(9), e2020WR028835.

Stewart, M. K., Mehlhorn, J., Elliott, S. (2007). Hydrometric and natural tracer (oxygen-18, silica, tritium and sulphur hexafluoride) evidence for a dominant groundwater contribution to Pukemanga Stream, New Zealand, *Hydrological Processes*, *21*, 3340–3356.

Stoelzle, M., Schuetz, T., Weiler, M., Stahl, K. & Tallaksen, L. M. (2020), Beyond binary baseflow separation. A delayed-flow index for multiple streamflow contributions, *Hydrology and Earth System Sciences*, *24*, 849–867. doi:10.5194/hess-24-849-2020

Stoelzle, M., Weiler, M., Stahl, K., Morhard, A. & Schuetz, T. (2014), Is there a superior conceptual groundwater model structure for baseflow simulation? *Hydrological Processes*, *29*, 1301–1313 doi:10.1002/hyp.10251

Szeftel, P., Moore, R. D. & Weiler, M. (2011), Influence of distributed flow losses and gains on the estimation of transient storage parameters from stream tracer experiments. *Journal of Hydrology*, *396*(3-4), 277–291.

Uhlenbrook, S. & Hoeg, S. (2003), Quantifying uncertainties in tracer-based hydrograph separations: a case study for two-, three-and five-component hydrograph separations in a mountainous catchment. *Hydrological Processes*, *17*(2), 431–453.

Voltz, T., Gooseff, M., Ward, A. S., Singha, K., Fitzgerald, M. & Wagener, T. (2013), Riparian hydraulic gradient and stream-groundwater exchange dynamics in steep headwater valleys, *Journal of Geophysical Research: Earth Surface*, *118*,953–969. doi:10.1002/jgrf.20074

Ward, A. S., Payn, R. A., Gooseff, M. N., McGlynn, B. L., Bencala, K. E., Kelleher, C. A., Wondzell, S. M. & Wagener, T. (2013), Variations in surface water-ground water interactions along a headwater mountain stream: Comparisons between transient storage and water balance analyses, *Water Resource Research*, *49*, 3359–3374. doi:10.1002/wrcr.2014

Ward, A. S., Wondzell, S. M., Schmadel, N. M., Herzog, S., Zarnetske, J. P., Baranov, V., Blaen, P. J., Brekenfeld, N., Chu, R., Derelle, R., Drummond, J., Fleckenstein, J. H., Garayburu-Caruso, V., Graham, E., Hannah, D., Harman, C. J., Hixson, J., Knapp, J. L. A., Krause, S., Kurz, M. J., Lewandowski, J., Li, A., Martí, E., Miller, M., Milner, A. M., Neil, K., Orsini, L., Packman, A. I., Plont, S., Renteria, L., Roche, K., Royer, T., Segura, C., Stegen, J., Toyoda, J., Wells, J. & Wisnoski, N. I. (2019), Spatial and temporal variation in river corridor exchange across a 5th-order mountain stream network, *Hydrology and Earth System Sciences*, *23*, 5199–5225, doi:10.5194/hess-23-5199-2019

Wels, C., Cornett, R. J. & Lazerte, B. D. (1991), Hydrograph separation: A comparison of geochemical and isotopic tracers. *Journal of Hydrology*, *122*(1-4), 253–274.

Wondzell, S. M. (2011), The role of the hyporheic zone across stream networks, *Hydrological Process*es, *25*, 3525–3532. doi:10.1002/hyp.8119

Wöhling, T., Wilson, S., Wadsworth, V., & Davidson, P. (2020), Detecting the cause of change using uncertain data: Natural and anthropogenic factors contributing to declining groundwater levels and flows of the Wairau Plain aquifer, New Zealand, *Journal of Hydrology*, *31*,100715, doi: 10.1016/j.ejrh.2020.100715

Zimmer, M. A. & McGlynn, B. L (2017), Bidirectional stream–groundwater flow in response to ephemeral and intermittent streamflow and groundwater seasonality. *Hydrological Processes, 31*, 3871-3880. doi:10.1002